Greene, P. J., Poonian, M. S., Nussbaum, A. L., Tobias, L., Garfin, D. E., Boyer, H. W., & Goodman, H. M. (1975) *J. Mol. Biol. 99*, 237–261.
Hines, J. L. (1979) Ph.D. Dissertation, The University of Chicago.
Hines, J. L., & Agarwal, K. L. (1979) *Fed. Proc., Fed. Am. Soc. Exp. Biol. 38*, 294.
Hines, J. L., Chauncy, T. R., & Agarwal, K. L. (1980) *Methods Enzymol. 65*, 153–163.
Jay, E., Bambara, R., Padmanabhan, R., & Wu, R. (1974) *Nucleic Acids Res. 1*, 331–353.
Marchionni, M. A., & Roufa, D. J. (1978) *J. Biol. Chem. 253*, 9075–9081.
Maxam, A., & Gilbert, W. (1977) *Proc. Natl. Acad. Sci. U.S.A. 74*, 560–564.
Model, P., & Zinder, N. D. (1974) *J. Mol. Biol. 83*, 231–251.
Modrich, P. (1979) *Q. Rev. Biophys. 12*, 315–369.
Modrich, P. (1980) *CRC Crit. Rev. Biochem.* (in press).
Panet, A., van de Sande, J. H., Lowen, P. C., Khorana, H. G., Raae, A., Lillehaug, J., & Kleppe, K. (1973) *Biochemistry 12*, 5045–5050.
Patel, D. J. (1979) *Eur. J. Biochem. 99*, 369–378.
Seeman, N. C., Rosenberg, J. M., & Rich, A. (1976) *Proc. Natl. Acad. Sci. U.S.A. 73*, 804–808.
Sgaramella, V., & Khorana, H. (1972) *J. Mol. Biol. 72*, 427–444.
Sharp, P. A., Sugden, B., & Sambrook, J. (1973) *Biochemistry 12*, 3055–3063.
Yoo, O. J. (1981) Ph.D. Dissertation, The University of Chicago.
Yoo, O. J., & Agarwal, K. L. (1980) *J. Biol. Chem. 255*, 6445–6449.

# Comparison of Transfer Ribonucleic Acid Structures Using Cobra Venom and $S_1$ Endonucleases†

Philip E. Auron, Lawrence D. Weber, and Alexander Rich*

ABSTRACT: Cobra venom nuclease $V_1$, which cleaves double-stranded RNA, has been used to study the structure of four *Escherichia coli* tRNAs: Phe, $Glu_2$, $Leu_2$, and $Ile_1$. The cleavage patterns are compared to those found for yeast $tRNA^{Phe}$, the three-dimensional structure of which is known. The cleavage patterns of all the tRNA molecules are similar, and the most sensitive cleavage is found at the central base pair of the anticodon stem. Studies of *E. coli* $tRNA_2^{Leu}$, which has a large variable loop, are consistent with the formation of a base-paired stem and loop structure that is not closely bound to the remainder of the molecule. A survey of the results suggests that the $V_1$ molecule may interact with the minor groove of the double helix with an affinity for stacked bases and that it may require two or three stacked bases for optimal binding and cleavage.

Enzymatic digestion has proved to be a valuable means of studying nucleic acid structure in solution, especially among transfer RNA (tRNA) molecules. Only a small number of tRNA species have been crystallized to date, and it has been difficult to obtain crystals of high quality. It is thus difficult to get direct structural information for many tRNA species. Although there is convincing evidence supporting the similarity between macromolecules in the crystalline state and their counterparts in solution (Chen et al., 1978; Matthews, 1974), such similarlity cannot be assumed to exist for all crystals or at all levels of detail. In this context, the enzymatic approach to structural study can both serve as a useful complement to high resolution crystallographic studies and provide significant structural information in solution for tRNA and other macromolecular species for which crystallographic information is unavailable.

Previous approaches to the enzymatic analysis of RNA structure have generally depended upon the use of single-strand-specific nucleases such as nuclease $S_1$ and ribonuclease $T_1$. The $S_1$ nuclease by itself is incapable of discerning all single-stranded regions within a nucleic acid molecule like tRNA. This is the case because some regions, such as the D and T loops, are held tightly together by tertiary interactions (Rich & Rajbhandary, 1976). Therefore, $S_1$ susceptibility testifies to a region's single-strandedness, but a lack of digestion is meaningless in deciding between secondary structure and tertiary structure. The use of other nucleases such as ribonucleases $T_1$ and A has proven successful in digesting $S_1$-resistant regions of some tRNA molecules; however, this is dependent upon the presence of specific residues within the region in question and is therefore not generally applicable.

The analysis of secondary structure in RNA molecules requires a method for determining the presence of double-stranded regions. Such information complements the $S_1$ and $T_1$ digestion data and can result in a more complete structural picture. An enzyme has been isolated from cobra venom that has the ability to cleave ribonucleic acid specifically within double-stranded regions (Vassilenko & Ryte, 1975). This enzyme, which has been called ribonuclease $V_1$ (Lockard & Kumar, 1981), can be used in concert with other digestion data for structure mapping tRNA molecules. Such an approach has been used in our laboratory and elsewhere to analyze the solution conformation of yeast $tRNA^{Phe}$, which has a known crystallographic structure. The results have indicated strong agreement between the X-ray crystal structure data and the enzymatic digestion pattern of this tRNA in solution (Lockard & Kumar, 1981). We have extended this enzymatic analysis

† From the Department of Biology, Massachusetts Institute of Technology, Cambridge, Massachusetts 02139. *Received March 12, 1982.* This work was supported by grants from the National Institutes of Health, the American Cancer Society, the National Science Foundation, and the National Aeronautics and Space Administration. P.A. was supported by Fellowship DRG-425F of the Damon Runyon-Walter Winchell Cancer Fund. L.W. was supported by National Research Service Award 3 F32 GM07078-01S1 BBCA and by Fellowship 61-525 of the Jane Coffin Childs Memorial Fund for Medical Research.

0006-2960/82/0421-4700$01.25/0 

to tRNA molecules lacking crystal structure determination, including a tRNA that possesses a long variable region. In this way we attempt to obtain structural information for these molecules and compare them with the structure of yeast $tRNA^{Phe}$. In addition, on the basis of the digestion pattern of several tRNA species, we can present a model that describes the $V_1$ substrate recognition.

## Materials and Methods

*Enzymes and Reagents.* Ribonucleases $T_1$ and A, calf alkaline phosphatase, $S_1$ nuclease, and T4 polynucleotide kinase were purchased from Boehringer-Mannheim. *Physarum* I ribonuclease was purchased from P-L Biochemicals, Inc. [$\gamma$-$^{32}$P]ATP (2300 Ci/mmol) was obtained from New England Nuclear Co. BD-cellulose was purchased from Boehringer-Mannheim, and Sepharose 4B and Sephadex G-75 were from Pharmacia Fine Chemicals. Plaskon, used in the preparation of RPC-5, was the generous gift of Dr. G. David Novelli, and the Adogen 464 was generously provided by Sherex Chemical Co., Inc.

*Isolation of tRNA.* Crude *Escherichia coli* tRNA was the generous gift of Dr. Karl Muench, University of Miami. The *E. coli* $tRNA_1^{Ile}$ used in this study was isolated in collaboration with Dr. S/awomir Bartkowiak, Institute for Plant Genetics, Polish Academy of Sciences, Poznan, Poland, who also prepared the RPC-5.

The crude tRNA was chromatographed by use of a column of benzoylated diethylaminoethylcellulose (BD-cellulose) after the method of Gillam et al. (1967). Crude fractions not containing Ile-charging activity were pooled at each step, precipitated with ethanol, redissolved in water, and stored frozen. Those column fractions containing Ile-charging activity were pooled and chromatographed by using Sepharose 4B according to the method of Holmes et al. (1975). The Ile-charging activity eluted as a single peak, the fractions of which were pooled and chromatographed by using RPC-5 chromatography at pH 7.5, after the method of Pearson et al. (1971) but at 20 °C. The Ile-charging activity eluted as two major peaks, the second one a doublet. The first peak was designated as Ile1 and rechromatographed in acetate buffer at pH 4.5. Two Ile-charging peaks were eluted, and these paralleled the $A_{260}$ profile. The first of these was designated $tRNA_{1A}^{Ile}$. Further purification by preparative gel electrophoresis was performed during the 5′-$^{32}$P end labeling procedure (see below), and the identity of this species as $tRNA_1^{Ile}$ was confirmed by examination of its partial digestion patterns with sequence-specific ribonucleases.

$tRNA^{Leu}$-charging activity was subsequently located in both the BD-cellulose and Sepharose 4B pooled fractions. The BD-cellulose fractions were rechromatographed, and a broad peak that contained the Leu-charging activity was pooled. This was chromatographed by using Sepharose 4B. The Leu-charging activity eluted as three peaks, one of which was large and well resolved. It eluted in the ammonium sulfate gradient at 0.57 M and paralleled a peak in the OD $A_{260}$ profile. These fractions were pooled and resolved into two bands by preparative gel electrophoresis (see below). The identity of each band was verified by sequence-specific partial digestion. The upper band was determined unambiguously to be $tRNA_2^{Leu}$.

*5′-$^{32}$P End Labeling of tRNA.* The methodology was essentially that of Wurst et al. (1978). Transfer RNA (1.5 $A_{260}$) was dissolved in 10 μL of 25 mM Tris-HCl, pH 8.0, and incubated for 30 min. at 60 °C with alkaline phosphatase. Following incubation, the enzyme was inactivated by addition of 1 μL of 50 mM nitrilotriacetic acid. This mixture was incubated at room temperature for 20 min, followed by 1 min at 100 °C. The tRNA was recovered by precipitation twice with a 2.5-fold volume of absolute ethanol. The resulting dephosphorylated tRNA was dissolved in water to a concentration of 0.1 $A_{260}$/mL, mixed with gel sample preparation buffer, and electrophoresed in a preparative polyacrylamide gel (see below).

The 5′-end labeling employed 0.12 $A_{260}$ dephosphorylated tRNA that was incubated with 82 pmol of [$\gamma$-$^{32}$P]ATP (2300 Ci/mmol) and 260 pmol of nonradioactive ATP in 8 μL of 25 mM Tris-HCl, pH 8.0, 10 mM $MgCl_2$, 6 mM 2-mercaptoethanol, 5% glycerol, 50 μg/mL bovine serum albumin, and 7.4 units of T4 polynucleotide kinase. This mixture was incubated at 37 °C for 60 min, followed by incubation at 100 °C for 1 min. The mixture was then diluted with an equal volume of electrophoresis sample preparation buffer and applied to a preparative polyacrylamide gel (see below).

*Polyacrylamide Electrophoresis.* Preparative gel electrophoresis (20 × 20 × 0.3 cm slabs) in 20% polyacrylamide–7 M urea–50 mM Tris–borate, pH 8.3, and recovery of RNA are described by Wrede et al. (1979a). Analytical polyacrylamide gel electrophoresis was similar to that used for preparative electrophoresis, except that the slab dimensions were 30 × 40 × 0.05 cm. Electrophoresis of analytical gels was at 1000 V. Gel sample preparation buffer consisted of 10 M urea, 5% glycerol, 0.05% bromophenol blue, and 0.05% xylene cylenol FF.

*Purification of the Double-Strand-Specific Ribonuclease from the Venom of the Central Asian Cobra. Naja oxiana* double-strand-specific ribonuclease (ribonuclease $V_1$) was purified according to the method of Vassilenko & Ryte (1975). Two grams of lyophilized venom from *Naja naja oxiana* (Sigma Chemical Co.) was dissolved to a volume of 12.3 mL, cleared by centrifugation at 15000 rpm, and dialyzed against 3 L (3 × 1 L) of 0.05 M Tris–succinate, pH 5.6. The volume following dialysis was 17.3 mL. Eleven milliliters of this solution was applied to a 93 × 2.5 cm column of Sephadex G-75 superfine equilibrated with 0.05 M Tris–succinate, pH 5.6. A flow rate of 6.2 mL/h was used, and 3-mL fractions were collected. Fractions were monitored for absorbance at 280 nm and assayed by degradation of 5-$^{32}$P-labeled yeast $tRNA^{Phe}$ (as determined by polyacrylamide gel electrophoresis) and by examination of fractions by $NaDodSO_4$–polyacrylamide gel electrophoresis using high cross-linker gels (Swank & Munkres, 1971). Fractions in the G-75 profile corresponding to the shoulder described by Vassilenko & Ryte (1975) were pooled (30 mL) and applied to a 1.5 × 45 cm column of Servacel SE23 (0.2–0.3 mequiv/g) sulfoethylcellulose (Accurate Chemical Corp.) that was equilibrated with 0.02 M Tris–succinate, pH 5.6. The column was eluted with a 700-mL linear gradient starting with 0.02 M Tris–succinate, pH 5.6, and ending with 0.02 M Tris, pH 10.1, containing 0.4 M NaCl. The flow rate was 15 mL/h, and 3.75-mL fractions were collected.

The nuclease activity was associated with fractions containing a $M_r$ 32400 protein. These fractions contained three minor protein contaminants, the molecular weights of which were determined to be 25700, 10000, and 5900. The assignment of 32400 to the nuclease activity was based on an alignment of the activity profile with the protein elution profile as judged by $NaDodSO_4$–polyacrylamide gel electrophoresis.

*Partial Digestion of tRNA.* Enzymatic partial digestions of 5′-$^{32}$P end-labeled tRNA were performed as follows. All digestions employed 0.045 $A_{260}$ (36000 cpm) of [$^{32}$P]tRNA unless stated otherwise. Following digestion, samples were mixed with an equal volume of gel sample preparation buffer.

Native digestions with $S_1$ nuclease used [5′-$^{32}$P]tRNA dissolved in 5 μL of 25 mM NaOAc, pH 4.5, 5 mM $MgCl_2$, and 50 mM KCl (native buffer). One microliter of a 5000 units/L solution of $S_1$ nuclease in 20 mM NaOAc (pH 4.5)–1 mM $Zn(OAc)_2$ was added to the solution, which was then incubated at 37 °C for 15–60 s. The reactions were terminated by rapid freezing in dry ice.

Nuclease $S_1$ digestions under denaturing conditions were similar to that described above, except that twice as much tRNA was used and the incubation was at 60 °C for 30 min.

Digestions employing ribonucleases $T_1$ and A under denaturing conditions used [5′-$^{32}$P]tRNA dissolved in 5 μL of 8 M urea–25 mM NaOAc (pH 4.5)–10 mM EDTA. One microliter of a 250 units/mL solution of ribonuclease $T_1$ in native buffer or 1 μL of a 1250 units/mL solution of ribonuclease A in native buffer was added, and the samples were incubated at 60 °C for 30 min.

Digestion with *Physarum* I ribonuclease employed [5′-$^{32}$P]tRNA dissolved in 5 μL of 25 mM NaOAc (pH 4.5)–1 mM EDTA (Simoncsits et al., 1977). One-tenth microliter of *Physarum* I ribonuclease was added to the mixture and incubated at 37 °C for 10 min.

Digestion of tRNA with ribonuclease $V_1$ used tRNA dissolved in 5 μL of native buffer to which was added 0.5 μL of the pooled $M_r$ 27 000 fractions described above. Incubation was at 25 °C. The reaction was terminated by rapid freezing in dry ice.

*Analysis of Digestion Patterns.* Nuclease $S_1$ and ribonuclease $V_1$ both cleave nucleic acids in such a manner that the resulting fragments possess 5′-phosphates at the cleavage site. This is distinct from cleavage by formamide, NaOH, or the enzymes ribonucleases $T_1$ and A and *Physarum* I, which yield 3′-phosphates at the site of cleavage.

This difference in product is a matter of concern in the analysis of polyacrylamide gel patterns in which comparison is made to a formamide digestion ladder. $S_1$ cleavage under denaturing conditions was used to construct a ladder with fragments possessing 5′-phosphates in order to make a less ambiguous assignment of $S_1$ and $V_1$ cleavage sites. Figure 1C (lanes 9) shows such an $S_1$ ladder. A comparison between this and the formamide ladder (lanes 6) illustrates the magnitude of the differences in migration rate for the two different classes of products. The difference is greatest when low molecular weight fragments are compared (positions 1–18) and less pronounced for the high molecular weight, more slowly moving bands. This behavior is consistent with the fact that 3′-phosphate 5′-end labeled fragments (derived from formamide cleavage) have a higher charge-to-mass ratio than $S_1$-derived fragments and that the charge-to-mass difference ratio between the two classes of fragments becomes less with increasing chain lengths.

## Results

*$V_1$ Nuclease Digestion of Representative tRNA Molecules.* Figure 1 shows "representative" structure mapping data for the tRNA molecules that were analyzed in this study. Interpretive drawings based on careful analysis of all gel data (including gels not shown here) are presented in Figure 2. Figure 2A represents a schematic summary of digestion results obtained for yeast $tRNA^{Phe}$ [data not shown, but see Lockard & Kumar (1981)]. The data fit the X-ray crystal structure extremely well (Kim et al., 1974; Quigley & Rich, 1976). Nuclease $S_1$ digestion is limited to the exposed anticodon loop (Wrede et al., 1979a,b), and nuclease $V_1$ digestion is limited to those regions that are known to be double stranded. No cleavage occurs at nucleotides that are not involved in the duplexes observed in the crystal. The lack of cleavage in certain double-stranded positions can be due to steric hindrance and perturbation of the duplex backbone by tertiary interactions.

Figure 2B–E shows the digestion patterns for several *E. coli* tRNA molecules. Although the consensus digestion pattern reflects the same cloverleaf theme as the yeast $tRNA^{Phe}$ structure, there appear to be some notable differences. The lack of digestion after (i.e., on the 3′ side of) nucleotide G4 in the yeast $tRNA^{Phe}$ acceptor stem is not apparent in any of the other tRNA molecules. This particular position in the yeast tRNA marks the location of a G–U base pair within the middle of the acceptor stem that appears to interfere with ribonuclease $V_1$ recognition. The fact that this position is cleaved in all the other tRNAs investigated that do not contain such a base pair at this position supports this idea.

Another difference observed between yeast $tRNA^{Phe}$ and the other tRNA molecules is in the digestion of sequence positions 8 and 9. Residues U8 and A9 in the yeast tRNA form base pairs, giving rise to tertiary interactions, and are not stacked with the D-stem and anticodon duplexes. The geometrical requirements of the U8–A14 and A9–A23 base pairs are such as to cause an abrupt departure from helicity in the sugar–phosphate backbone in the U8 region. On the basis of sequence considerations, U8 and U9 of *E. coli* $tRNA^{Phe}$ and $tRNA^{Ile}$ are probably involved in similar tertiary interactions, rendering them relatively protected from $V_1$ cleavage. However, in *E. coli* $tRNA_2^{Glu}$ and $tRNA_2^{Leu}$ there is increased susceptibility of the 8 and 9 positions to $V_1$ ribonuclease. In both these tRNA molecules the 9–23 interaction is unlikely, if a geometry that is essentially similar to that of yeast $tRNA^{Phe}$ is assumed, and perhaps some arrangement occurs that organizes these nucleotides into a structure reflecting quasi-double-helical character, such as a stacked conformation. Additionally, both of these molecules diverge from the yeast $tRNA^{Phe}$ structure in that the D loop contains at least one extra nucleotide. In the case of $tRNA_2^{Leu}$ the situation is more complicated since the D stem is closed on the D-loop side by a purine–purine (G–A) base pair. These structural differences might relate to those observed in the $V_1$ digestion patterns.

The anticodon stem–loop region digestion patterns for several tRNAs are compared in Figure 3. The only similarity that is apparent among the molecules studied is the common cleavage site after residue 28, which is independent of nucleotide sequence. In the examples shown all four nucleotides are represented at position 28, and all appear to be cleaved equally well. This position is located within the center of the anticodon stem stack (see Figure 4) and probably represents a fairly stable region of the structure. Cleavage at other positions along the 5′ side of the anticodon stem seems to be somewhat dependent upon the nature of the nucleotides present. In this regard the enzyme appears to have a preference for G- and C-stacked residues. In particular, as observed for $tRNA_1^{Ile}$ and $tRNA_2^{Glu}$, cleavage actually extends into the anticodon loop. Remarkably, cleavage on the 5′ side of the anticodon stem is generally greater than that of the 3′ side.

In summary, the $V_1$ results are largely similar among the tRNA species studied but with a few important differences. We find that we are able to understand many of these differences by extrapolation from the known structural data.

*$S_1$ Nuclease Digestion of E. coli $tRNA_2^{Leu}$.* Figure 2D also indicates the result of $S_1$ nuclease treatment of *E. coli* $tRNA_2^{Leu}$ under native conditions. Digestion is limited to only

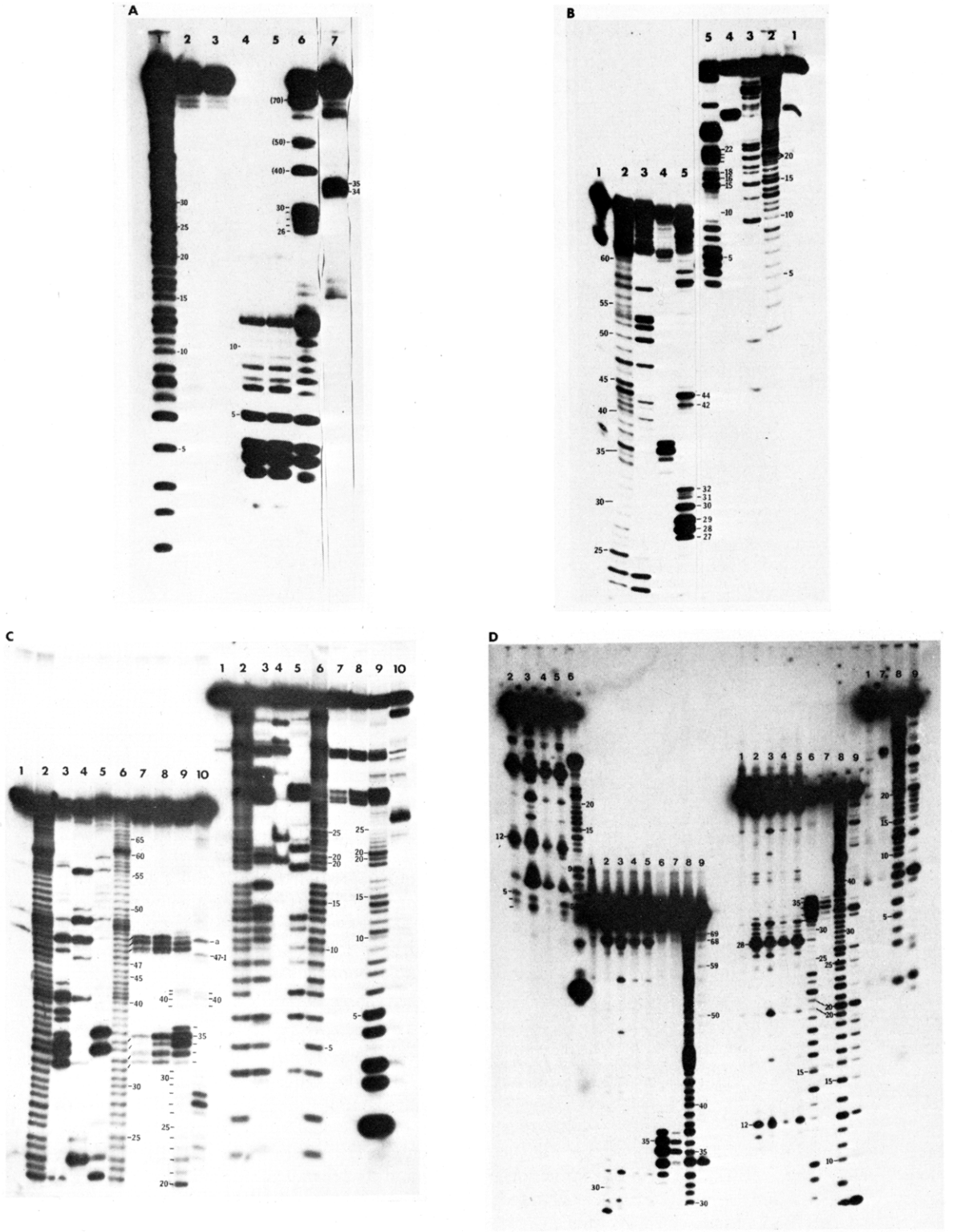


FIGURE 1: Autoradiograms of 5′-$^{32}$P-labeled *E. coli* tRNA molecules electrophoresed on 20% polyacrylamide as described in the text. Sequence position assignments in parentheses are approximate and not indicated in Figure 2. (A) $tRNA^{Phe}$: 1, formamide ladder; 2, minus enzyme control; 3, minus enzyme control; 4, ribonuclease $V_1$ (37 °C, 1 min); 5, ribonuclease $V_1$ (37 °C, 5 min); 6, ribonuclease $V_1$ (25 °C, 30 s); 7, nuclease $S_1$ (37 °C, 1 min). Additional lanes in the original autoradiogram between 6 and 7 were removed as the material was repetitious. (B) $tRNA_2^{Glu}$: 1, minus enzyme control; 2, formamide ladder; 3, ribonuclease $T_1$; 4, nuclease $S_1$ (60 °C, 30 min); 5, ribonuclease $V_1$ (25 °C, 30 s). (C) $tRNA_2^{Leu}$: 1, minus enzyme control; 2, formamide ladder; 3, ribonuclease *Physarum* I; 4, ribonuclease A; 5, ribonuclease $T_1$; 6, formamide ladder; 7, nuclease $S_1$, (37 °C, 10 s); 8, nuclease $S_1$ (37 °C, 60 s); 9, nuclease $S_1$ (60 °C, 30 min); 10, ribonuclease $V_1$ (25 °C, 5 min). The "a" indicates a $Mg^{2+}$-sensitive cleavage site that is also present in the minus enzyme control lane (lane 1). (D) $tRNA_1^{Ile}$: 1, minus enzyme control; 2, ribonuclease $V_1$ (25 °C, 5 s); 3, ribonuclease $V_1$ (25 °C, 25 s); 4, ribonuclease $V_1$ (1:10 dilution; 25 °C, 20 s); 5, ribonuclease $V_1$ (1:10 dilution; 25 °C, 2 min); 6, nuclease $S_1$ (60 °C, 30 min); 7, nuclease $S_1$ (37 °C, 1 min); 8, formamide ladder; 9, ribonuclease $T_1$.

two regions that correspond to the anticodon and variable arm of this class II tRNA (a class II tRNA is one possessing a long variable loop). The anticodon loop cleavage is similar to that observed for elongator class I tRNA molecules (Wurst et al., 1978; Wrede et al., 1979a,b). These investigators have demonstrated that native class I tRNA molecules are cleaved by

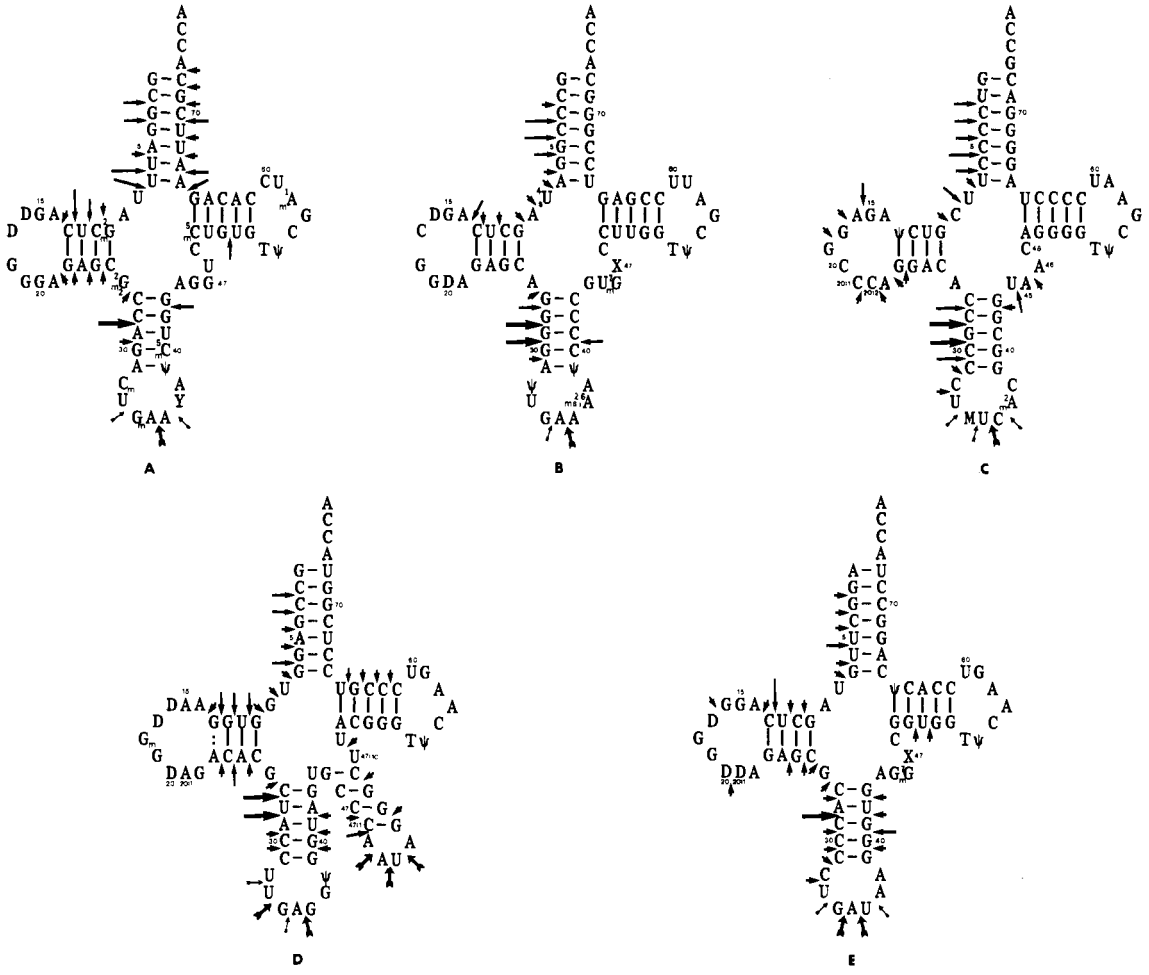

FIGURE 2: Secondary structure diagrams of tRNA molecules indicating nuclease-sensitive sites. Tailless arrows indicate ribonuclease $V_1$ sites. Tailed arrows indicate nuclease $S_1$ sensitive sites. The size of the arrow is proportional to the cleavage intensity. (A) Yeast $tRNA^{Phe}$ [data not shown, but see Lockard & Kumar (1981)]; (B) *E. coli* $tRNA^{Phe}$; (C) *E. coli* $tRNA_2^{Glu}$; (D) *E. coli* $tRNA_2^{Leu}$; (E) *E. coli* $tRNA_1^{Ile}$.

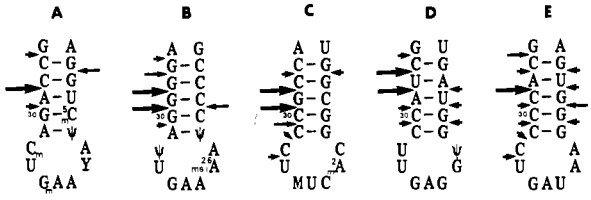

FIGURE 3: Comparison of the anticodon stem–loop region indicating ribonuclease $V_1$ sensitive sites. The arrow size is proportional to the cleavage intensity. Labels A–E correspond to labels A–E in Figure 2.

$S_1$ nuclease only in the anticodon loop and not in either the D or T loops, presumably because of tertiary interactions between these two regions. Furthermore, it was demonstrated that for the elongator tRNA molecules, cleavage would occur at many sites within the anticodon loop. This pattern for noninitiator tRNA molecules appears to be conserved in this class II tRNA. The variable arm cleavage is limited to three sites within the presumably four-membered loop bounded by a putative C47:1–G47:6 base pair (see Figure 2C). These sites, which are on the 3′ side of residues A47:2, A47:3, and A47:4, appear to be equally susceptible to nuclease $S_1$.

The pattern of $S_1$ digestion observed within the variable arm region of this tRNA molecule appears to be consistent with the secondary structure shown in Figure 2. Furthermore, the similarity between the cleavage pattern of the variable loop and that of the anticodon loop implies that both possess similar degrees of exposure to the solvent, thus indicating that the variable loop, unlike the D and T loops, is not excluded by tertiary interactions from digestion by $S_1$. In other experiments (not shown) we have found that nuclease $S_1$ digestion of yeast mitochondrial $tRNA_2^{Leu}$ yielded similar results in that the variable loop is also cleaved.

## Discussion

*tRNA Structural Comparison Based on $V_1$ Digestion Patterns.* In order to understand the manner in which nuclease $V_1$ cleaves the double-stranded regions of tRNA molecules we would like to know the geometry of the interactions between these two molecules. Unfortunately, we know the structure of only one member of the pair. However, it should be borne in mind that the nuclease with a molecular weight of 32 400 is comparable in size to the tRNA molecule substrates. The contact region between the two molecules may thus cover a significant distance along the polynucleotide chain and not necessarily the same distance in the 3′ and 5′ directions. Furthermore, the enzyme could make contact in the grooves, even though it appears not to be sequence dependent. Digestion is found in the D stem in which the major groove is almost entirely filled with bases from other parts of the molecule; this suggests that the enzyme is unlikely to bind to the major groove.

Our results have demonstrated the structural sensitivity of the $V_1$ enzyme, and they are consistent with the widely accepted view of the basic structural homology of different tRNA species. This is emphasized in Figure 4, which shows the base stacking of yeast $tRNA^{Phe}$ as deduced from the X-ray structure

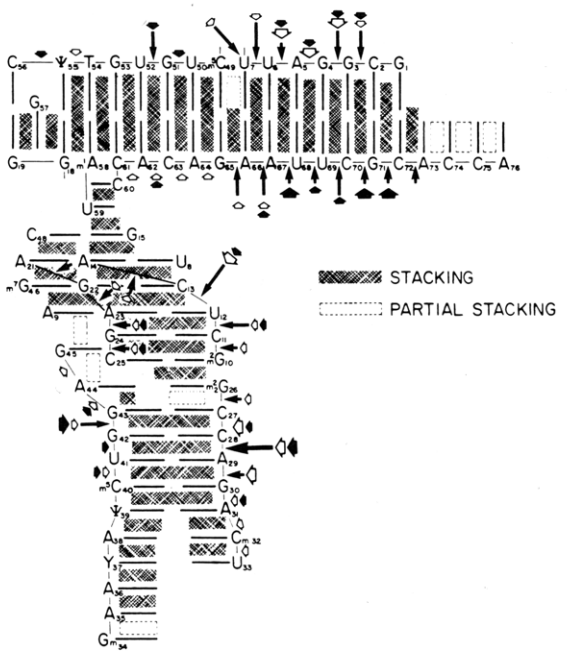


FIGURE 4: Base-stacking diagram of yeast $tRNA^{Phe}$ as determined by X-ray diffraction (Kim et al., 1974). Thin arrows correspond to nuclease $V_1$ sensitive sites in yeast $tRNA^{Phe}$ (see Figure 3A). Broad open arrows correspond to a ribonuclease $V_1$ consensus cleavage pattern for the *E. coli* tRNA molecules presented in this paper superimposed upon the yeast $tRNA^{Phe}$ structure for comparison purposes. Broad closed arrows correspond to a consensus cleavage pattern for human $tRNA_i^{Met}$ and *E. coli* $tRNA_f^{Met}$ reported by Lockard & Kumar (1981), also for comparison to yeast $tRNA^{Phe}$. The arrow size is proportional to the cleavage intensity.

(Kim et al., 1974). It also summarizes results for ribonuclease $V_1$ digestion of several elongator and initiator tRNA molecules. The acceptor and T stems represent the longest, most exposed, and uniform duplex structure in the molecule. The acceptor stem is a prime target for this enzyme, while the T stem, which is also a uniform helix, is not as good a substrate. This is perhaps due to the steric constraints imposed by its proximity to the remainder of the tRNA molecule. In particular, the major groove of the T stem is virtually blocked due to the adjacent D stem. In the anticodon stem, position 28 is located at the center of a uniform stretch of five contiguous stacked base pairs, and it is highly sensitive to ribonuclease $V_1$.

The enzymatic digestion data that we have presented reveal some interesting structural features of tRNA molecules that have not yet been analyzed by X-ray crystallography. *E. coli* $tRNA_2^{Leu}$ is a class II tRNA molecule possessing a variable loop with sufficient length to form a base-paired stem. The $S_1$ nuclease pattern for this tRNA, as well as that for *Neurospora crassa* mitochondrial $tRNA_2^{Leu}$, indicates that the region of the long variable loop judged to be single stranded on the basis of primary sequence was readily accessible to $S_1$ cleavage. This implies a variable loop conformation in which this region is exposed and thus lends experimental credence to a variable loop base-paired region as represented in the structural model for *E. coli* $tRNA^{Ser}$ proposed by Brennan & Sundaralingam (1976). By contrast, $V_1$ is less active in the base-paired region of the variable loop and least active on the 3′ side. This may suggest that the stem is folded back on the molecule, protecting much of it from digestion. Alternatively, access to this region by the enzyme might be affected by bulky neighboring groups. Nonetheless, the cleavage at positions 47 and 47:1, as well as the slight susceptibility of positions 47:6 and 47:8, is consistent with the existence of a duplex in this part of the molecule.

Another tRNA that has not been examined X-ray crystallographically is $tRNA_2^{Glu}$. This is the only class I tRNA observed to have a very sensitive $V_1$ site at position U8, and it possesses four rather than five nucleotides within the variable loop. In yeast $tRNA^{Phe}$, U8 is adjacent to the variable loop. An X-ray crystallographic structure has been presented for yeast $tRNA^{Asp}$ (Moras et al., 1980), which also has a four-nucleotide variable loop. In that structure the shorter variable loop results in a significantly higher solvent exposure for position U8 compared to yeast $tRNA^{Phe}$, which has five variable loop nucleotides. This might account for the observed cleavage in $tRNA_2^{Glu}$. The only other tRNA that appears to be very sensitive to U8 cleavage is *E. coli* $tRNA^{Leu}$, a class II (long variable arm) tRNA. It is possible that the long variable arm is oriented in a direction away from U8, leaving the latter exposed for enzymatic cleavage. However, U8 seems unlikely to be positioned where it is a good candidate for strong ribonuclease $V_1$ cleavage judging from the yeast $tRNA^{Phe}$ structure.

*A Model for $V_1$ tRNA Recognition.* $V_1$ digestion experiments for the tRNAs we have discussed reveal some interesting features in the manner in which the enzyme recognizes its substrate. Although cleavage is restricted primarily to double-stranded regions, it is not associated with any particular nucleotide or nucleotide sequence. The only apparent feature in common between the different cleavage patterns (Figure 2) is position 28. This represents one of the most intensely cleaved sites in all the tRNA molecules used in this study. Similar strong cleavage has been observed at this position for yeast $tRNA^{Val}$ (Favorova et al., 1981) and *E. coli* $tRNA_f^{Met}$ and human $tRNA_i^{Met}$ (Lockard & Kumar, 1981). Preliminary studies on *E. coli* $tRNA_{Su^-}^{Trp}$ in our laboratory also reinforce this observation. Whatever the enzyme recognizes in tRNA substrates appears to be most uniformly associated with this location. However, it is not nucleotide sequence since the sequence diversity at this location is large. The only obvious similarity relates to the location of position 28 at the center of the anticodon stem.

The data that we have presented support the notion that the enzyme recognizes a stretch of the RNA duplex. Position 28 might represent an especially good substrate due to its stacking interactions with other base pairs on both sides of it in the helix. A specificity toward such stacked regions might also explain the fact that for all tRNAs studied to date, the acceptor end is a prime target for $V_1$ attack. This is the largest region of continuous stacking (see Figure 4).

The preference for stacked nucleotides may also account for the limited single-strand digestion seen at positions 31 and 32 in both *E. coli* $tRNA_1^{Ile}$ and $tRNA_2^{Glu}$. Stacking is found at a similar place in the yeast $tRNA^{Phe}$ crystal structure. The fact that only two tRNAs showed sensitivity to $V_1$ at those sites might be related to the stabilizing influence of particular types of nucleotide stacking arrangements. Tinoco et al. (1973) have tabulated free energy values for different types of nucleic acid stacking. The cleavage patterns observed, especially on the 5′ side of the anticodon stem and the occasional single-strand cleavage of the anticodon loop, correlated with these free energy values. There is a direct relationship between high nuclease sensitivity and the absolute magnitude of the calculated free energy for the affected stem region. It is also apparent that the reduced sensitivity after position G4 in yeast $tRNA^{Phe}$ marks the location of a G–U base pair. Such base pairs do not stack well, according to the Tinoco rules. Interestingly, the G4 in yeast $tRNA^{Phe}$ is slightly farther away from the helix axis than in a normal Watson–Crick base pair,

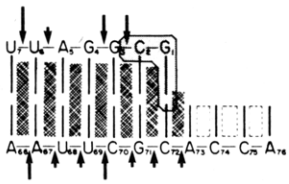

FIGURE 5: A portion of the base-stacking diagram of yeast $tRNA^{Phe}$ showing only yeast $tRNA^{Phe}$ specific ribonuclease $V_1$ cleavage sites. The stippled L-shaped region represents a minimum active site for ribonuclease $V_1$ that is consistent with the data (see that text for details).

while U69 is closer (Quigley & Rich, 1976), yet the sugar–phosphate backbone helical geometry remains relatively undistorted (G. J. Quigley, personal communication).

The reduced cleavage after G4, taken with the crystallographic observation of an undistorted backbone, can be used as an argument against a mechanism of recognition by which $V_1$ relies exclusively on backbone conformation. It is thus reasonable to assume that the enzyme must also interact with a helical groove in effecting recognition and cleavage. Further, the digestion patterns reveal cleavage sites on both strands of specific duplexes but they only occur in one position at a time. The cleavage event appears to be a single-strand nick and not a double-strand break as is found in many DNA restriction endonucleases. This is consistent with a model in which the enzyme binds specifically to only one phosphate–sugar backbone.

The enzyme seems to lack the ability to discriminate among the various types of bases. This may support recognition in the minor groove and not the major groove. The H-bond donor–acceptor environment within the major groove of an RNA duplex is not symmetric for a particular base pair, nor is it the same for two different base pairs (Seeman et al., 1976). The major groove is thus an ideal binding site for proteins that require a large degree of sequence specificity. On the other hand, the minor groove presents a very uniform and symmetric disposition of H-bond acceptors. This provides a reasonable recognition surface for an enzyme such as $V_1$ that does not show sequence specificity. In addition, cleavage never seems to occur after position 1. This can be incorporated into a model for enzyme recognition in which $V_1$ binds to a stacked duplex site but cleaves at least one nucleotide ahead toward the 3′ side of the backbone.

A schematic minimum model of the active site region of ribonuclease $V_1$ is presented in Figure 5. It is a minimum model because the enzyme may recognize a larger region of the stem, but only this part is essential to describe the observed results. The active site is represented as a shaded L-shaped region in which recognition of hydrogen-bond acceptors and donors within the minor groove is associated with nucleolytic cleavage at a position on the backbone that is one nucleotide removed from the recognition site. This model is consistent with virtually all the observed tRNA cleavage sites. In fact, the cleavages at positions U8 and A45 in *E. coli* $tRNA_2^{Glu}$ can now be explained simply, as resulting from overcutting into the single-stranded regions. In the case of A45 the enzyme may utilize the potential base pair at A26–U44 to effect overcutting. A model such as this may be useful in interpreting future experiments with $V_1$ ribonuclease.

## Acknowledgments

We thank Lorren Yee, Gary Quigley, Joyce Heckman, Regina Reilly, and Lee Gehrke for advice and discussions, Sławomir Bartkowiak for isolation of bacterial tRNAs, and Linda J. Swanson for excellent technical assistance.

## References

Brennan, T., & Sundaralingam, M. (1976) *Nucleic Acids Res. 3*, 3235–3251.

Chen, M. C., Giege, R., Lord, R. C., & Rich, A. (1978) *Biochemistry 17*, 3134–3138.

Favorova, O. O., Fasiolo, F., Keith, G., Vassilenko, S. K., & Ebel, J.-P. (1981) *Biochemistry 20*, 1006–1011.

Gillam, J., Millward, I., Blew, D., von Tigerstram, M., Wimmer, E., & Tener, G. M. (1967) *Biochemistry 6*, 3043–3056.

Holmes, W. M., Hurd, R. E., Reid, B. R., Rimerman, R. A., & Hatfield, G. W. (1975) *Proc. Natl. Acad. Sci. U.S.A. 72*, 1068–1071.

Kim, S. H., Sussman, J. L., Suddath, F. L., Quigley, G. J., McPherson, A., Wang, A. H.-J., Seeman, N. C., & Rich, A. (1974) *Proc. Natl. Acad. Sci. U.S.A. 71*, 4970–4974.

Lockard, R. E., & Kumar, A. (1981) *Nucleic Acids Res. 9*, 5125–5140.

Matthews, B. W. (1974) *The Proteins* (Neurath, H., & Hill, R. L., Eds.) 3rd ed., Academic Press, New York.

Moras, D., Comarmond, M. B., Fischer, J., Weiss, R., & Thierry, J. C. (1980) *Nature (London) 288*, 669–674.

Pearson, R. L., Weiss, J. F., & Kelmers, A. D. (1971) *Biochim. Biophys. Acta 228*, 770–774.

Quigley, G. J., & Rich, A. (1976) *Science (Washington, D.C.) 194*, 796–806.

Rich, A., & Rajbhandary, U. (1976) *Annu. Rev. Biochem. 45*, 805–860.

Seeman, N. C., Rosenberg, J. M., & Rich, A. (1976) *Proc. Natl. Acad. Sci. U.S.A. 73*, 804–808.

Simoncsits, A., Brownlee, G. G., Brown, J. R., & Guilley, H. (1977) *Nature (London) 269*, 833–836.

Swank, R. T., & Munkres, K. D. (1971) *Anal. Biochem. 39*, 462.

Tinoco, I., Borer, P. N., Dengler, B., Levine, M. D., Uhlenbeck, O. C., Crothers, D. M., & Gralla, J. (1973) *Nature (London), New Biol. 246*, 40–41.

Vassilenko, S. K., & Ryte, V. K. (1975) *Biokhimiya (Moscow) 40*, 578–583.

Wrede, P., Woo, N. H., & Rich, A. (1979a) *Proc. Natl. Acad. Sci. U.S.A. 76*, 3289–3293.

Wrede, P., Wurst, R., Vournakis, J., & Rich, A. (1979b) *J. Biol. Chem. 254*, 9608–9616.

Wurst, R. M., Vournakis, J. N., & Maxam, A. M. (1978) *Biochemistry 17*, 4493–4499.